



Universiteit
Leiden
The Netherlands

Copper complexes as biomimetic models of catechol oxidase: mechanistic studies

Koval, I.A.

Citation

Koval, I. A. (2006, February 2). *Copper complexes as biomimetic models of catechol oxidase: mechanistic studies*. Retrieved from <https://hdl.handle.net/1887/4295>

Version: Corrected Publisher's Version

License: [Licence agreement concerning inclusion of doctoral thesis in the Institutional Repository of the University of Leiden](#)

Downloaded from: <https://hdl.handle.net/1887/4295>

Note: To cite this publication please use the final published version (if applicable).

Dinuclear Cu^{II} complexes with the new phenol-based ligand bearing pyridine and thiophene substituents: synthesis, characterization and interaction with catechol substrates.[†]

The reaction of the phenol-based ligand 2,6-bis[*N*-(2-pyridylmethyl)-*N*-(2-thiophenylmethyl)aminomethyl]-4-methylphenol (Hpy2th2s), containing pyridine and thiophene substituents, with copper(II) chloride and bromide yields two new dinuclear complexes of composition $[\text{Cu}_2(\text{py2th2s})(\mu\text{-X})\text{X}_2]$, where X = Cl or Br. In both complexes, the copper(II) ions are pentacoordinated and bridged by the deprotonated phenolate anion and by one halogen anion. Both complexes exhibit geometric asymmetry, as the coordination environment around one of the two copper ions is square-pyramidal, whereas the other can be best described as a distorted trigonal bipyramid. The complexes were characterized by means of X-ray single-crystal diffraction, ligand field, EPR and mass spectroscopy and electrochemistry. Magnetic susceptibility measurements indicate an antiferromagnetic coupling between two metal centers ($2J \approx -200 \text{ cm}^{-1}$). The interaction of the complexes with model substrates 3,5-di-*tert*-butylcatechol and tetrachlorocatechol is reported.

[†]This chapter is based on: Koval, I. A., Huisman, M., Stassen, A. F., Gamez, P., Roubeau, O., Belle, C., Pierre, J. L., Saint-Aman, E., Luken, M., Krebs, B., Lutz, M., Spek, A. L., Reedijk, J., *Eur. J. Inorg. Chem.*, 2004, 4036-4045

4.1 Introduction

As discussed in Chapter 1, an interesting structural feature encountered in the active site of catechol oxidase from sweet potatoes (*Ipomoea batatas*)¹ is an unusual thioether bond between a carbon atom of one of the histidine ligands and the sulfur atom of a nearby cysteine residue from the protein backbone. This structural moiety is thought to impose additional structural restraints on the coordination sphere of one of the copper ions, which may in turn optimize the redox potential of the metal needed for the oxidation of the catechol substrate and may allow a rapid electron transfer in the redox processes. Although a very large number of synthetic models of the type-3 active site appeared in literature in the past few decades, relatively little attention has been paid to this thioether bond.² In an attempt to mimic this quite unusual structural feature a new dinucleating phenol-based ligand 2,6-bis[*N*-(2-pyridylmethyl)-*N*-(2-thiophenylmethyl)aminomethyl]-4-methylphenol (abbreviated as Hpy2th2s) with two pendant arms, containing pyridine and thiophene residues, was prepared.

Recent studies on the copper complexes of HL_R ligands, published by Belle *et al.*³ (see Chapter 1), allowed to propose a new catalytic mechanism for catechol oxidation, emphasizing the role of the μ -hydroxo bridge between the two metal centers. It includes the monodentate coordination of the substrate to one of the metal centers with the concomitant cleavage of the OH bridge, and the subsequent proton transfer from the second OH group of the catechol substrate to the hydroxyl group bound to the second copper center.³ The release of a water molecule results in a bridging coordination of the catecholate, which undergoes an oxidation to quinone. In order to further demonstrate the importance of the μ -hydroxo bridge on the catalytic cycle, two dinuclear copper(II) complexes with Hpy2th2s have been synthesized, and their structural, spectroscopic, magnetic and electrochemical properties along with their interaction with the model substrates, 3,5-di-*tert*-butylcatechol (DTBCH₂) and tetrachlorocatechol (TCC), have been investigated. In these complexes, the two metal ions are doubly bridged by the oxygen atom of the phenolate group and a halogen anion. The influence of the bridging ligands (*e.g.* a halogen *vs.* the hydroxyl anion) on the catecholase activity of dicopper(II) complexes is discussed.

4.2 Results and Discussion

4.2.1 Synthesis

The synthesis of this ligand is depicted in Figure 4.1. The starting compound for the ligand synthesis, *N*-(2-pyridylmethyl)-*N*-(2-thiophenylmethyl)amine, was prepared by reacting the commercially available 2-formylthiophene and 2-methylpyridilamine followed by the reduction of the *in situ* generated imine by NaBH₄. The starting compound 2,6-bis(chloromethyl)-4-methylphenol was prepared as previously described.⁴ The reaction of 2,6-bis(chloromethyl)-4-methylphenol with a stoichiometric

amount of *N*-(2-pyridylmethyl)-*N*-(2-thiophenylmethyl)amine, in the presence of an excess of NEt_3 , resulted in the formation of the ligand, which was isolated as a transparent light-yellow oil. The reaction of Hpy2th2s with copper(II) chloride and bromide led to the formation of two new dinuclear copper complexes, which were isolated as a dark-brown and dark-purple crystals, respectively.

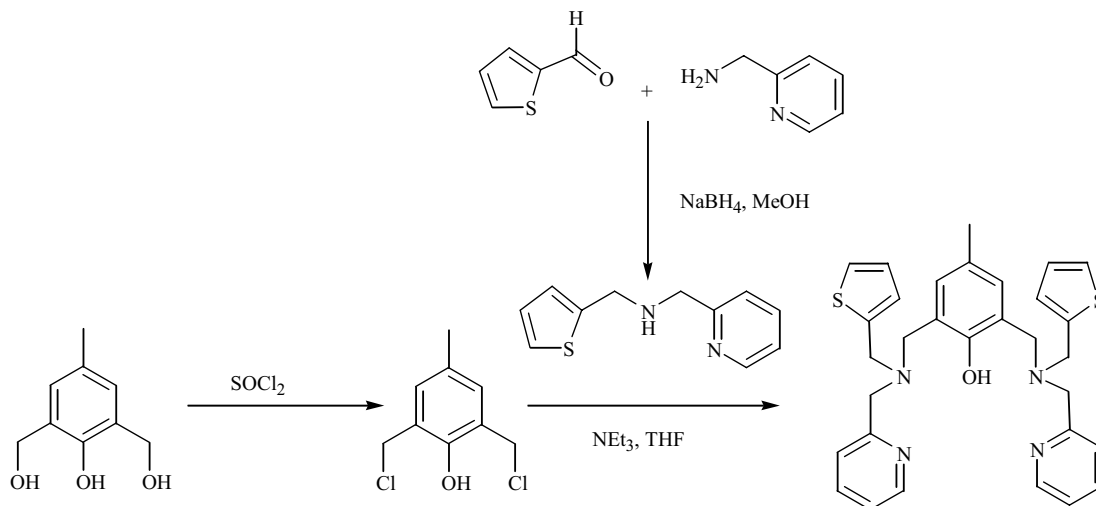


Figure 4.1. The reaction scheme of the synthesis of Hpy2th2s

4.2.2 Crystal structure descriptions

$[\text{Cu}_2(\text{py}2\text{th}2\text{s})(\mu\text{-Cl})\text{Cl}_2]\cdot\text{CH}_3\text{OH}$ (**1**)

Rectangular reddish-brown crystals of the complex **1** were obtained by diethyl ether diffusion into a methanol solution containing stoichiometric amounts of copper(II) chloride and the ligand. An ORTEP projection of the crystal structure of the complex is shown in Figure 4.2. Selected bond lengths and angles are presented in Table 4.1.

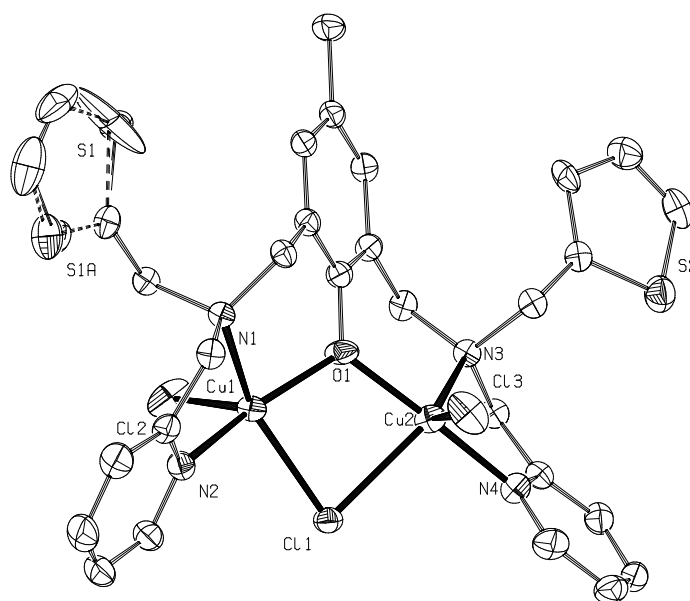


Figure 4.2. ORTEP projection of the complex $[\text{Cu}_2(\text{py}2\text{th}2\text{s})(\mu\text{-Cl})\text{Cl}_2]\cdot\text{CH}_3\text{OH}$ (**1**). Hydrogen atoms and a non-coordinated methanol molecule are omitted for clarity.

Table 4.1. Selected bond lengths and bond angles of the complex [Cu₂(py2th2s)(μ -Cl)Cl₂] \cdot CH₃OH (**1**)

<i>Bond lengths (Å)</i>			
Cu1 - O1	1.9209(19)	Cu2 - O1	1.911(2)
Cu1 - N2	1.975(2)	Cu2 - N4	1.972(2)
Cu1 - N1	2.103(2)	Cu2 - N3	2.083(2)
Cu - Cl1	2.3922(8)	Cu2 - Cl1	2.4717(9)
Cu1 - Cl2	2.3931(10)	Cu2 - Cl3	2.3636(10)
Cu1 - Cu2	3.185(1)		
<i>Bond angles (°)</i>			
O1 - Cu1 - N2	159.33(9)	O1 - Cu2 - N4	168.80(9)
O1 - Cu1 - N1	90.47(8)	O1 - Cu2 - N3	90.59(8)
N2 - Cu1 - N1	81.53(9)	N4 - Cu2 - N3	82.01(9)
O1 - Cu1 - Cl1	82.70(6)	O1 - Cu2 - Cl1	80.76(6)
N2 - Cu1 - Cl1	95.90(7)	N4 - Cu2 - Cl1	97.76(7)
N1 - Cu1 - Cl1	153.25(6)	N3 - Cu2 - Cl1	131.18(6)
O1 - Cu1 - Cl2	100.79(7)	O1 - Cu2 - Cl3	94.77(7)
N2 - Cu1 - Cl2	99.74(7)	N4 - Cu2 - Cl3	96.43(7)
N1 - Cu1 - Cl2	106.18(6)	N3 - Cu2 - Cl3	130.53(6)
Cl1 - Cu1 - Cl2	100.50(3)	Cl1 - Cu2 - Cl3	98.17(4)

The complex crystallizes as methanol solvate in space group $P2_1/n$, with four formula units present per unit cell. The dinuclear core is constituted by two copper(II) ions, bridged on the one side by the endogenous cresolato bridge and on the other side by the chloride anion. The Cu...Cu separation in the complex is 3.185(1) Å. Both copper(II) ions are pentacoordinated with the identical N₂OCl₂ donor sets. However, the complex possesses geometrical asymmetry, as the coordination geometry around Cu1 is almost a regular square pyramid ($\tau = 0.10$),⁵ whereas the coordination environment around the Cu2 ion can be best described as a heavily distorted trigonal bipyramid ($\tau = 0.63$).⁵ The basal plane of the square pyramid around the Cu1 ion is constituted by the nitrogen atom N1 of the tertiary amine group, the N2 atom of the pyridine ring, the oxygen atom O1 of the cresolate moiety, and the bridging chloride atom Cl1, whereas another chloride anion Cl2 occupies the apical position. In the case of the Cu2 ion, the nitrogen atom N3 of the tertiary amine group, the bridging chloride atom Cl1 and the chloride atom Cl3 form the equatorial plane of the trigonal bipyramid. The axial positions are occupied by the nitrogen atom N4 of the pyridine ring and the oxygen atom O1 of the cresolate group. The thiophene rings of the ligand remain non-coordinated; the Cu...S separations are > 5 Å. One of the thiophene rings shows disorder, with the sulfur atom being refined on two independent positions, with

occupancy factors of 78% (S1) and 22% (S1a). One non-coordinated disordered methanol molecule is present per formula unit, which is hydrogen-bonded to the chloride atom Cl3 (the distance Cl3...O2 = 3.077 Å, the distance Cl3...O2a = 3.179 Å).

[Cu₂(py2th2s)(μ-Br)Br₂] (2)

Very dark purple needles of the complex **2** were obtained by slow evaporation of an acetonitrile solution containing stoichiometric amounts of copper(II) bromide and the ligand. An ORTEP projection of the crystal structure is shown in Figure 4.3. Selected bond lengths and angles are presented in Table 4.2.

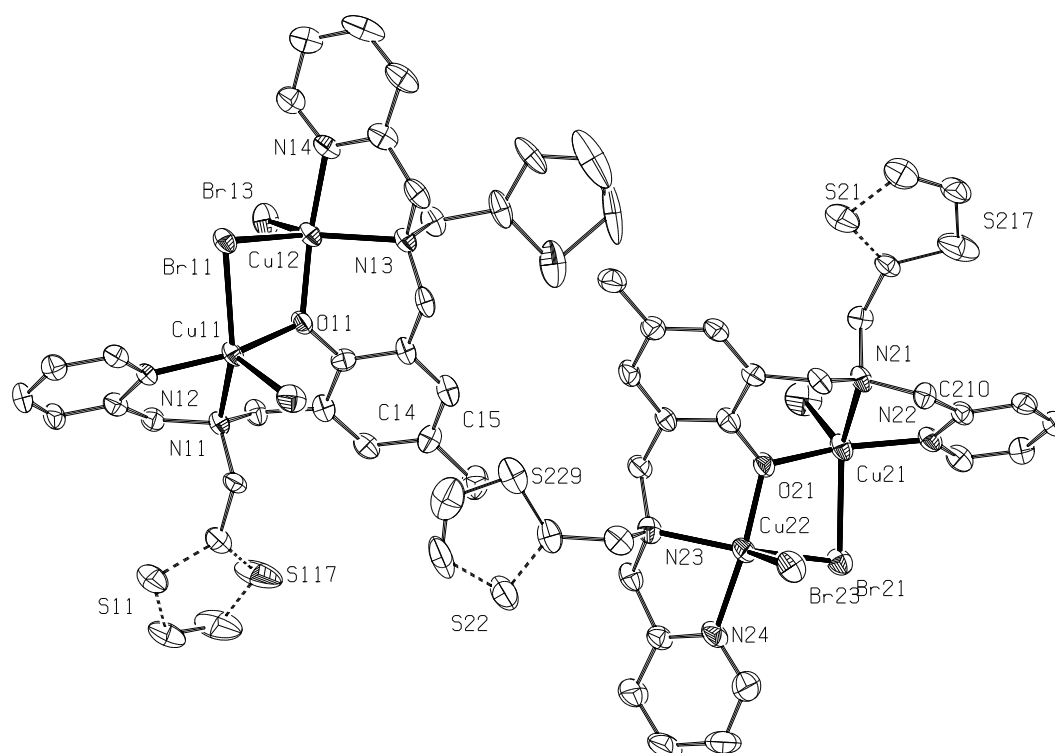


Figure 4.3. ORTEP projection of the two independent formula units of [Cu₂(py2th2s)(μ-Br)Br₂] (**2**).

Hydrogen atoms are omitted for clarity. Three of the thiophene rings are rotationally disordered.

The complex crystallizes in space group $P\bar{1}$. The asymmetric unit consists of two independent formula units. As in the case of the chloride complex **1**, two copper(II) ions are doubly bridged by the oxygen atom of the cresolate moiety and the halogen anion. The Cu...Cu distances are 3.2710(10) and 3.2394(10) Å, respectively. Both copper ions are pentacoordinated, with N₂OBr₂ donor sets. One of the two independent formula units (Cu11, Cu12) possesses geometrical asymmetry. The geometry around the Cu11 ion is a slightly distorted square pyramid ($\tau = 0.17$),⁵ whereas the geometry around the Cu12 ion is a significantly distorted trigonal bipyramid ($\tau = 0.58$).⁵

Table 4.2. Selected bond lengths and bond angles of the complex [Cu₂(py2th2s)(μ -Br)Br₂] (**2**).

<i>Bond distances (Å)</i>			
Cu11 - O11	1.925(3)	Cu12 - O11	1.931(4)
Cu11 - N12	1.977(4)	Cu12 - N14	1.986(5)
Cu11 - N11	2.099(4)	Cu12 - N13	2.096(4)
Cu11 - Br11	2.5620(9)	Cu12 - Br11	2.5226(8)
Cu11 - Br12	2.5314(8)	Cu12 - Br13	2.4870(9)
Cu21 - O21	1.931(3)	Cu22 - O21	1.918(4)
Cu21 - N22	1.968(4)	Cu22 - N24	1.981(5)
Cu21 - N21	2.112(4)	Cu22 - N23	2.113(4)
Cu21 - Br21	2.5535(10)	Cu22 - Br21	2.5666(9)
Cu21 - Br22	2.5166(9)	Cu22 - Br23	2.4953(9)
Cu11 - Cu12	3.2710(10)	Cu21 - Cu22	3.2394(10)

<i>Bond angles (°)</i>			
O11 - Cu11 - N12	159.37(17)	O11 - Cu12 - N14	165.93(17)
O11 - Cu11 - N11	91.14(16)	O11 - Cu12 - N13	91.70(17)
N11 - Cu11 - N12	81.55(17)	N13 - Cu12 - N14	81.61(19)
Br11 - Cu11 - O11	81.00(11)	Br11 - Cu12 - O11	81.95(10)
Br11 - Cu11 - N12	95.53(13)	Br11 - Cu12 - N14	93.07(13)
Br11 - Cu11 - N11	149.47(13)	Br11 - Cu12 - N13	130.96(12)
Br12 - Cu11 - O11	97.77(11)	Br13 - Cu12 - O11	96.52(11)
Br12 - Cu11 - N12	102.84(12)	Br13 - Cu12 - N14	97.54(13)
Br12 - Cu11 - N11	108.72(13)	Br13 - Cu12 - N13	119.60(12)
Br11 - Cu11 - Br12	101.58(3)	Br11 - Cu12 - Br13	109.44(3)
O21 - Cu21 - N22	162.14(18)	O21 - Cu22 - N24	164.78(18)
O21 - Cu21 - N21	91.15(16)	O21 - Cu22 - N23	90.99(17)
N21 - Cu21 - N22	81.54(17)	N23 - Cu22 - N24	81.71(19)
Br21 - Cu21 - O21	83.16(12)	Br21 - Cu22 - O21	83.04(11)
Br21 - Cu21 - N22	93.90(14)	Br21 - Cu22 - N24	93.39(15)
Br21 - Cu21 - N21	146.37(13)	Br21 - Cu22 - N23	137.81(12)
Br22 - Cu21 - O21	99.57(12)	Br23 - Cu22 - O21	95.20(11)
Br22 - Cu21 - N22	98.26(13)	Br23 - Cu22 - N24	99.98(14)
Br22 - Cu21 - N21	110.29(13)	Br23 - Cu22 - N23	122.65(12)
Br21 - Cu21 - Br22	103.34(3)	Br21 - Cu22 - Br23	99.51(3)
Cu11 - O11 - Cu12	116.04(18)	Cu21 - O21 - Cu22	114.63(19)
Cu11 - Br11 - Cu12	80.08(3)	Cu21 - Br21 - Cu22	78.50(3)

The nitrogen atom N11 of the tertiary amine group, the nitrogen atom N12 of the pyridine ring, the bridging oxygen atom O11 and the bridging bromide anion Br11 are forming the basal plane of the square pyramid around the Cu11 ion, whereas the monocoordinated bromide anion Br12 is occupying the axial position. The equatorial plane of the trigonal bipyramid around the Cu12 ion is formed by the nitrogen atom N13 of the tertiary amine group and the bromide atoms Br11 and Br13. The axial positions of the bipyramid are occupied by the bridging oxygen atom of the cresolate group and the nitrogen atom N14 of the pyridine ring. One of the non-coordinated thiophene rings is rotationally disordered. Thus, the first orientation has an occupancy factor of 85%, while the 180° rotated orientation has an occupancy factor of 15%. In the second independent formula unit, both copper(II) ions (Cu21 and Cu22) have a significantly distorted square pyramidal geometry ($\tau = 0.26$ for the Cu21 ion and 0.45 for the Cu22 ion)⁵. The basal plane around the Cu21 ion is constituted, similarly to the Cu11 ion, by the two nitrogen atoms N21 and N22, the oxygen atom O21 of the cresolate group and the bridging halogen atom Br21, whereas the bromide anion Br22 occupies the apical position. For the Cu22 ion, the nitrogen atom N23 of the tertiary amine group, the nitrogen atom N24, the bridging oxygen atom O21 and the bridging bromide atom Br21 are forming the basal plane of the square pyramid, with its apical position being occupied by the Br23 atom. Thus, two square pyramids share one side through the atoms O21 and Br21, with their apical positions *trans* located to each other. Both thiophene rings of the ligand remain non-coordinated (Cu...S separations are > 5 Å) and exhibit rotational disorder. Thus, the thiophene ring at S21 was refined on two orientations with occupancies of 0.72 and 0.28, respectively, and the thiophene ring at S22 with occupancies of 0.55 and 0.45, respectively.

4.2.3 Physical characterization

4.2.3.1 Ligand field spectroscopy

The ligand field spectra of both complexes, recorded in the solid state (diffuse reflectance), exhibit almost identical features. Both spectra are characterized by the presence of the charge transfer band from the phenolate moiety to the copper ions⁶ around 500 nm (483 nm for complex **1** and 521 nm for complex **2**), and the d-d transition band of the copper(II) ions. The latter band, observed at 774 nm for the chloride complex and at 806 nm for the bromide complex, is in both cases asymmetric, with a shoulder observed at higher wavelengths. As shown previously, such spectroscopic behavior (high-energy absorption band in the visible region with a low-energy shoulder) is typical for square-pyramidal copper(II) complexes.⁷ In acetonitrile solution, the charge transfer band is observed at 472 nm for complex **1** ($\epsilon = 1851 \text{ M}^{-1}\text{cm}^{-1}$) and at 500 nm for complex **2** ($\epsilon = 1812 \text{ M}^{-1}\text{cm}^{-1}$). The d-d band is located at 771 nm ($\epsilon = 464 \text{ M}^{-1}\text{cm}^{-1}$) for complex **1** and 791 nm ($\epsilon = 534 \text{ M}^{-1}\text{cm}^{-1}$) for complex **2**.

A small shift of the d-d bands upon dissolution of the complexes in acetonitrile may suggest the coordination of the solvent to the metal centers. However, the partial dissociation of the complexes due to the exchange of the halide anions with acetonitrile molecules can also not be excluded.

4.2.3.2 EPR and magnetic susceptibility studies

Both complexes **1** and **2** are EPR silent in the solid state and in a frozen acetonitrile solution at 100 K, suggesting an antiferromagnetic coupling between the copper ions. Such a behavior is confirmed by the temperature dependence of the molar magnetic susceptibility χ_M depicted in Figure 4.4, which is typical for complexes of antiferromagnetically coupled copper(II) dimers. Indeed the χ_M vs. T curves present a broad maximum centered around 160 and 190 K for **1** and **2** respectively, while the values of χ_M at high temperatures (2.10×10^{-3} and 1.85×10^{-3} cm³ mol⁻¹ at 300 K respectively) are slightly lower than expected for two uncoupled copper(II) ions (2.5×10^{-3} cm³ mol⁻¹ for $g = 2$). Below 40 K, a Curie tail ascribed to paramagnetic impurities is observed, which is usual in such copper(II) complexes. These experimental data were reproduced correctly using the modified Bleaney-Bowers equation (4.1) where χ_M is the magnetic susceptibility per dimer.

$$\chi_M = (1 - \rho) \frac{2N_A \beta^2 g^2}{k_B T} \left[\frac{1}{3} + \exp(-2J / k_B T) \right]^{-1} + 2\rho \left(\frac{N_A \beta^2}{k_B T} \right) + TIP \quad (4.1)$$

In this equation, $2J$ corresponds to the singlet-triplet energy gap, ρ the fraction of paramagnetic impurity and TIP a term to account for temperature independent paramagnetism, while N_A , β , k_B and g have their usual meaning. The paramagnetic impurity was assumed to be a mononuclear copper(II) species and g was fixed to 2. The best fit parameters were then obtained as $2J = -177(2)$ cm⁻¹, $\rho = 1.8(1)\%$ and $TIP = 2.9(1) \times 10^{-4}$ cm³ mol⁻¹ for complex **1** and $2J = -219(1)$ cm⁻¹, $\rho = 0.6(1)\%$ and $TIP = 2.0(1) \times 10^{-4}$ cm³ mol⁻¹ for complex **2**. These medium antiferromagnetic couplings should be correlated to a significant overlap between the two magnetic orbitals of the two copper(II) ions in complexes **1** and **2**, through both the halide and phenolate bridges. The short Cu-O bonds and the large Cu-O-Cu angles of the phenolate bridge in **1** and **2**, compared to the long Cu-X bonds, point at a dominant coupling through the phenolate bridge. The coordination sphere around one of the two copper ions is intermediate between a square pyramid and a trigonal bipyramid, while the other has a square pyramidal environment. In the former case, the unpaired electron of copper(II) occupies either the d_z^2 or the $d_{x^2-y^2}$ orbital, which would both point along the Cu-O(phenolate) bond. Short Cu-O bonds and large Cu-O-Cu angles in square pyramidal phenolate bridged Cu dimers result in a strong overlap of $d_{x^2-y^2}$ orbitals and thus produce strong to very strong antiferromagnetic couplings.⁸ On the other hand, if one of the copper ions in

such dimers has a trigonal bipyramidal environment, a weaker overlap is expected, and even a weak ferromagnetic coupling has been observed in some cases.^{9,10} Therefore, the smaller singlet-triplet energy gap in **1** can be related either to a smaller Cu-O-Cu angle in **1** (*ca.* 112°), compared to **2** (on average over the two dimeric units *ca.* 115.3°), but also to a more distorted trigonal bipyramid coordination sphere in **2** ($\tau = 0.58$, Cu12) than in **1** ($\tau = 0.63$, Cu2). Most likely the difference in the singlet-triplet energy gap is resulting from both structural differences.

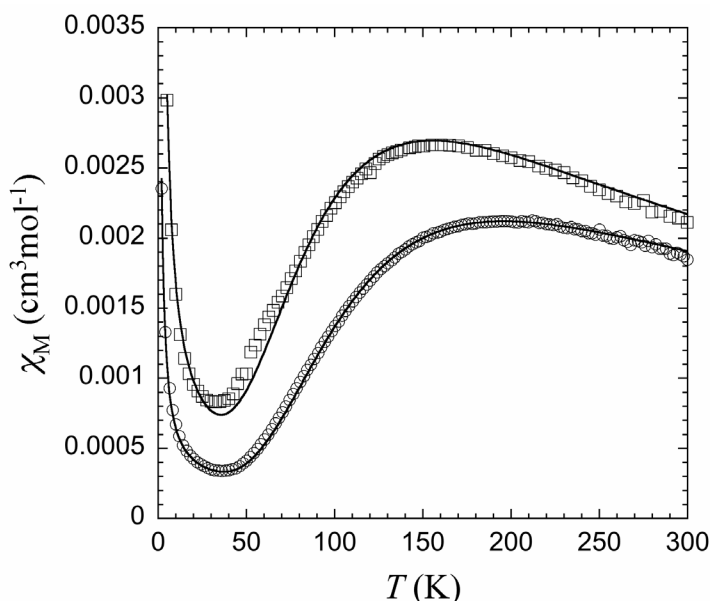


Figure 4.4. χ_M vs. T curve for complexes **1** (□) and **2** (○).

4.2.3.3 Electrochemistry

The electrochemical behavior of both complexes was investigated by cyclic voltammetry (CV) and rotating disk electrode voltammetry (RDE) in acetonitrile solution, with tetra-*n*-butylammonium perchlorate (TBAP) as supporting electrolyte (0.1 M). The potentials are referred to an Ag/10mM AgNO₃ + CH₃CN + 0.1 M TBAP reference electrode.

When scanning towards the negative region of potentials, the CV curve for both complexes **1** and **2** is characterized by three successive electrochemical signals (Figures 4.5 and 4.6). While the first one for **1**, at $E_{pc} = -0.52$ V, is irreversible, re-oxidation of the reduced species being seen on the reverse scan at +0.23 V (Figure 4.5, curve a), for **2** it appears to be quasi reversible with $E_{1/2} = -0.34$ V ($\Delta E_p = 0.12$ V, Figure 4.6, curve a). Coulometric titrations give $n = 1$ exchanged electron per complex, allowing to attribute this electrochemical system to the complexed Cu^{II,II}₂/Cu^{II,I}₂ redox couple. The UV-Vis spectra of the one-electron reduced complexes exhibit one very broad band around 680 nm. The lack of reversibility of the first electrochemical reduction of **1** and **2** suggests a change in the coordination sphere around the metal center upon reduction, likely a partial dissociation of the exogenous halide ligand and a change in the geometry

of the coordination sphere. Additional electrochemical measurements performed at $-40\text{ }^{\circ}\text{C}$ showed that the course of these coupled chemical reaction is not prevented at low temperature. The second electrochemical signal, quasi reversible with $E_{1/2} = -0.78\text{ V}$ for **1** and at $E_{1/2} = -0.72\text{ V}$ for **2**, corresponds as well to a one-electron process, leading to the complexed $\text{Cu}^{\text{II,I}}_2/\text{Cu}^{\text{I,I}}_2$ redox couple. Finally, the third electrochemical signal at $E_{\text{pc}} = -1.45\text{ V}$ for **1** and -1.04 V for **2** corresponds to a two-electron process, suggesting the reduction of Cu^{I} ions to the Cu^0 state and the deposition of metallic copper on the electrode surface. Accordingly, an additional sharp anodic peak is observed on the reverse scan, caused by the redissolution of the metallic copper.

The anodic behavior of complexes **1** and **2** differs. The anodic part of the CV curve for **1** (Figure 4.5, b) is characterized by two electrochemical signals, whereas three signals are observed on the CV curve for **2** (Figure 4.6, b). For **1**, the first one at $E_{1/2} = 0.64\text{ V}$ ($\Delta E_{\text{p}} = 0.26\text{ V}$) corresponds to a one-electron quasi-reversible oxidation of the complex. The electron transfer is likely to be centered on the phenolate bridge, as previously shown for other phenolate-bridged dinuclear copper(II) complexes.^{6,11} This process is followed by the oxidation of the chloride anions which is seen as a shoulder at the negative foot of the over-oxidation wave of the complex (free chloride anions are reversibly oxidized at 0.72 V under the current experimental conditions).

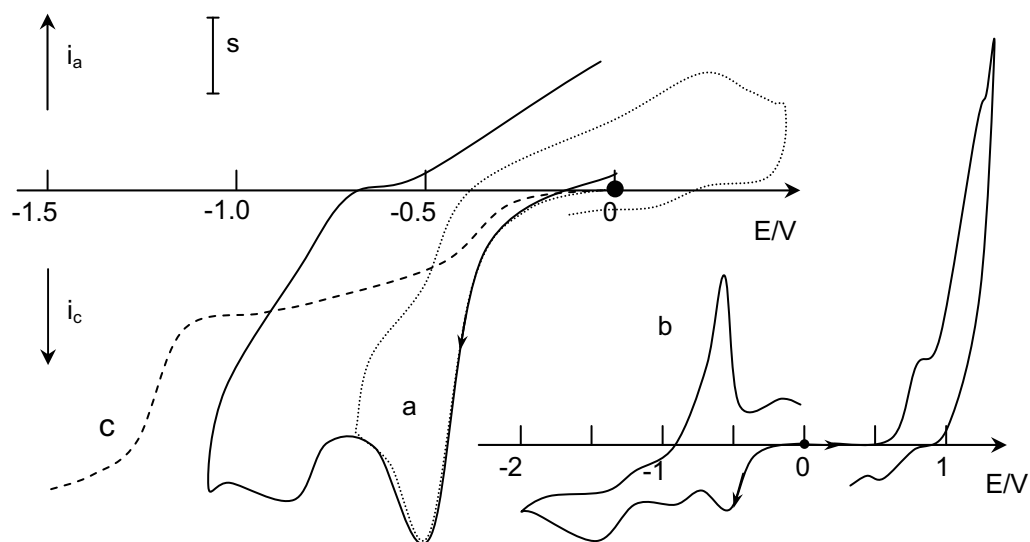


Figure 4.5. Electrochemical curves recorded in a 0.67 mM solution of **1** in $\text{CH}_3\text{CN} + \text{TBAP } 0.1\text{ M}$ on a Pt disc ($\varnothing = 5$ (a, b) or 3 (c) mm); curves a, b: CV curves, $v = 0.1\text{ V s}^{-1}$; curve c: RDE curve, $N = 600\text{ rpm}$; V vs $\text{Ag}/\text{AgNO}_3\text{ mM} + \text{CH}_3\text{CN} + \text{TBAP } 0.1\text{ M}$. Scale $s = 20\text{ }\mu\text{A}$ (curve a), $120\text{ }\mu\text{A}$ (curve b) or $10\text{ }\mu\text{A}$ (curve c)

The CV curve recorded in a solution of **2** shows an additional fully irreversible one-electron system at $E_{\text{pa}} = 0.47\text{ V}$. It is assumed to be due to the one-electron oxidation of bromide anions, free bromide anions being irreversibly oxidized at $E_{\text{pa}} = 0.39\text{ V}$ under the current experimental conditions. The one-electron, phenolate-based,

oxidation of the complex **2**, similarly to **1**, is observed as a quasi-reversible pair of peaks at $E_{1/2} = 0.76$ V ($\Delta E_p = 0.18$ V) and is followed at higher potentials by the over-oxidation of the complex.

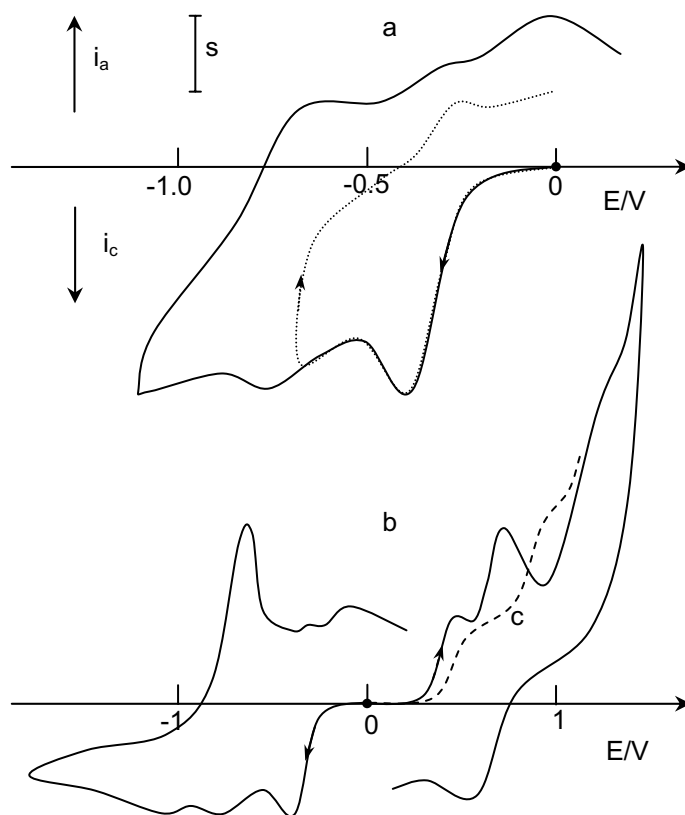


Figure 4.6. Electrochemical curves recorded in a 0.67mM solution of **2** in $\text{CH}_3\text{CN} + \text{TBAP}$ 0.1 M on a Pt disc ($\varnothing = 5$ (a, b) or 3 (c) mm); curves a, b: CV curves, $v = 0.1 \text{ V s}^{-1}$; curve c: RDE curve, $N = 600 \text{ rpm}$; V vs Ag/AgNO_3 mM + $\text{CH}_3\text{CN} + \text{TBAP}$ 0.1 M. Scale $s = 20 \mu\text{A}$ (curve a), $40 \mu\text{A}$ (curve b, c).

These results have been confirmed by rotating disk electrode (RDE) voltammetry experiments (Figures 4.5 and 4.6, dashed lines). The RDE curves display one anodic wave at $E_{1/2} = 0.84$ V for **1** and two successive well-behaved anodic waves at $E_{1/2} = 0.42$ V and 0.82 V (Figure 4.6, curve c) for **2**. For both complexes, three successive cathodic waves are seen. For **1** and **2**, the first one at $E_{1/2} = -0.42$ V and -0.40 V, respectively, is followed by a second ill-behaved wave at $E_{1/2} = -0.78$ V and -0.80 V respectively. The third cathodic wave corresponding to the deposition of metallic copper onto the electrode surface is observed at $E_{1/2} = -1.22$ V and -1.20 V, respectively.

4.2.3.4 Conductivity measurements

The conductivity measurements of the complexes **1** and **2** were performed on 0.5 mM solutions of the complexes in acetonitrile. The calculated values for equivalent conductivities of both compounds are roughly the same and are equal to $52 \text{ cm}^2 \cdot \text{mol}^{-1} \cdot \text{Ohm}^{-1}$ for complex **1** and $55 \text{ cm}^2 \cdot \text{mol}^{-1} \cdot \text{Ohm}^{-1}$ for complex **2**. Previously, the conductivity range for complexes corresponding to 1:1 type electrolytes was

suggested to lie between 120 and 160 $\text{cm}^2\cdot\text{mol}^{-1}\cdot\Omega\text{m}^{-1}$, if acetonitrile was utilized as a solvent.¹² Although values as low as 90 $\text{cm}^2\cdot\text{mol}^{-1}\cdot\Omega\text{m}^{-1}$ were also reported in some cases, the observed conductivities of both complexes **1** and **2** are still too low to address them as 1:1 electrolytes. As shown previously,¹³ such small conductivity values are often found in acetonitrile for non-electrolytes, due to coordinating and solvating properties of this solvent. Some authors¹³ argue that they may indicate a partial exchange of counter anions with solvent molecules. Small changes in the positions of the UV-Vis-NIR d-d bands of the complexes upon their dissolution in acetonitrile, observed in the present case, appear to sustain this assumption.

4.2.4 Interaction of the complexes with the model substrates

4.2.4.1 Catecholase activity measurements

To evaluate the ability of the complexes to behave as functional models of catechol oxidase, they were tested as catalysts in the oxidation of 3,5-di-*tert*-butylcatechol (DTBCH₂), a widely used model substrate, to the respective quinone. Both complexes exhibit only negligible catecholase activity (TON < 1 after 30 min), making a detailed kinetic analysis dispensable. These results are as expected, confirming that the substitution of the μ -hydroxo bridge by a halogen anion precludes the catecholase activity. However, these results do not provide information whether or not the binding of the substrate to the metal centers *at all* takes place. Reim *et al.*¹⁴ have previously shown that, in the case of essentially inactive complexes, no interaction between the dimetal core and the substrate occurred (see Chapter 1). To evaluate whether or not the first step of the catalytic cycle, *e.g.* the binding of catechol to the metal centers, takes place, the interaction of the complexes with tetrachlorocatechol (TCC) was studied. The latter catechol has a very high oxidation potential due to its electron-withdrawing substituents, and is not oxidized by copper complexes.

4.2.4.2 TCC binding studies

The titration of $5\cdot 10^{-4}$ M solutions of the complexes in acetonitrile with TCC was followed by means of UV-Vis and EPR spectroscopy. The changes observed in UV-Vis spectra of complex **1** upon addition of TCC (up to 4 equivalents) are depicted in Figure 4.7, left. Quite significant changes in the spectrum of the original complex indicate the interaction between the substrate and the metal centers. The presence of two isosbestic points at 570 nm and 724 nm shows the occurrence of only two absorbing species in solution. The Cu^{II} d-d transition band shifts gradually from 789 nm to 718 nm, whereas its absorption decreases to *ca.* 50% of its initial value. Also, the extinction coefficient of the LMCT band decreases from 1851 to *ca.* 1600 $\text{M}^{-1}\text{cm}^{-1}$ (Figure 4.7).

Whereas the chloride complex obviously reacts with TCC, no changes in the UV-Vis spectrum were observed upon addition of TCC to the bromide complex. Taking

into account a very large structural similarity between the two complexes, it seems reasonable to suggest that the difference in their behavior is caused by the different halogen anions, coordinated to the copper ions. The Cu-Cl bond has a more ionic character in comparison with the Cu-Br bond, which therefore facilitates the substitution of (at least one of) the chloride anions by catechol, whereas no exchange of Br anions with TCC occurs.

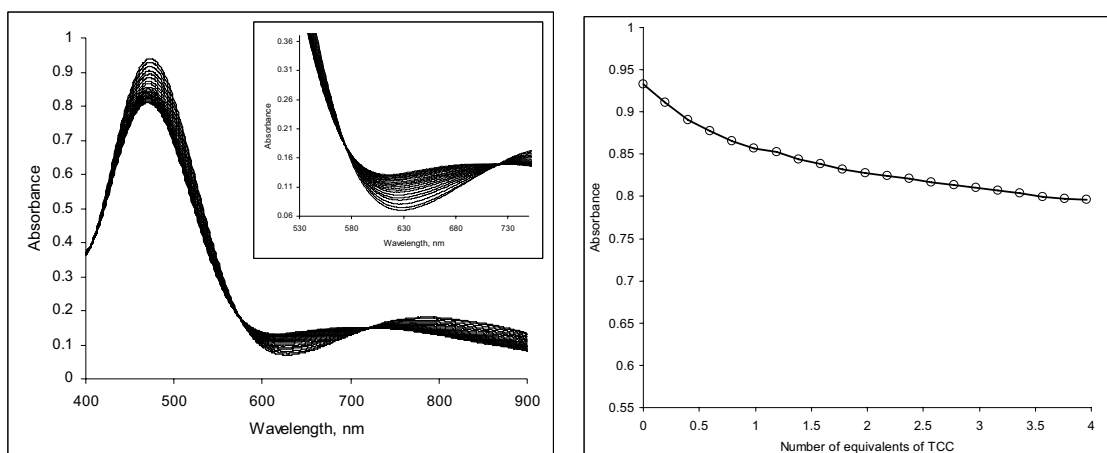


Figure 4.7. Left: UV-Vis titration of the complex **1** (0.5 mM solution in acetonitrile) with TCC (from 0 to 4 equivalents). The insert shows the enlargement of the spectroscopic curves in the range 530-780 nm. Right: decrease of the LMCT band (474 nm) upon titration of the solution of **1** (0.5 mM) in acetonitrile with TCC.

A titration of complex **1** with TCC, followed by X-band EPR spectroscopy, revealed that no evolution of the EPR signal is observed upon addition of TCC. This indicates that the two copper ions are strongly antiferromagnetically coupled, suggesting that they probably remain doubly bridged by the phenolate group and the chloride anion. Although a few structures of copper(II) complexes with a bridging catecholate were previously described,^{15,16} no magnetic properties of these compounds have been reported. However, it can be proposed that the cleavage of the halide bridge would lead to the decrease in strength of the magnetic coupling, similarly to the behavior of previously reported μ -hydroxo complexes with phenol-based ligands³ after the cleavage of the hydroxo bridge. Thus, the reaction of TCC with the chloride complex results probably in the substitution of at least one of the apical chloride anions. In order to further confirm this hypothesis the conductivity of complex **1** in acetonitrile solution before and after an addition of TCC was studied. The equivalent conductivity of TCC itself in CH₃CN is negligible.

The values of the equivalent conductance, observed after addition of 1-4 equivalents of TCC to a 0.5 mM solution of complex **1** are listed in Table 4.3. As can be seen, a substantial increase in conductivity is observed after one equivalent of TCC has been added. Further addition of TCC leads to a slight increase of conductivity, till a

final value of $118 \text{ cm}^2 \cdot \text{mol}^{-1} \cdot \text{Ohm}^{-1}$ is reached. This value fits perfectly in the range suggested for 1:1 electrolytes in acetonitrile.¹² The interaction of **1** with TCC leads to the release of one chloride anion in solution, the complete release being reached in the presence of an excess of TCC as shown by the slight increase of the conductivity above one molar equivalent added. The reversible character of this process is further confirmed from UV-Vis titration experiments that showed that the maximal perturbation in the UV-Vis spectra was reached in the presence of at least 3 equivalents of TCC (Figure 4.7).

Not surprisingly, additions of TCC to the bromide complex do not lead to an increase in conductivity, which is in complete agreement with the hypothesis that no substitution of Br^- anions with TCC is possible.

Table 4.3. Changes in the equivalent conductivity of a 0.5 mM solution of **1** in acetonitrile upon treatment with TCC

<i>Number of equivalents of TCC</i>	<i>Equivalent conductivity ($\text{cm}^2 \text{ mol}^{-1} \text{ Ohm}^{-1}$)</i>
0	52
1	100
2	110
3	117
4	118

4.2.5 General discussion

Many attempts to establish a correlation between the structural parameters of the complexes and their catalytic activity in the oxidation of catechols have been described in literature. Three most important criteria influencing the catalytic properties of the complexes can now be distinguished: (i) the distance between the metal centers,^{6,17,18} (ii) the nature of the bridging group between the metal ions,^{19,20} (iii) the electronic properties of the complexes.¹¹ Some other factors, *e.g.* the imposed strain in the complex, due to the rigidity of either the ligand and/or the bridging group, may also play a role.¹⁴ Results published by Reim *et al.*¹⁴ (see Chapter 1) indicate that complexes with strained structures show catalytic activity, whereas complexes present in relaxed, energetically favored conformation are essentially inactive towards catechol oxidation. In the chloride and bromide complexes **1** and **2**, the metal-metal distance and the redox potentials of the metal ions are comparable with the values previously determined for catalytically active complexes,^{6,14,19} thus, the absence of catalytic activity is not likely to be due to these two factors. Also, the coordination spheres around the copper ions in both complexes exhibit quite a large distortion from a regular square-pyramidal geometry, resulting in relatively

strained structures. Thus, the main reason for the absence of catalytic activity must originate from the nature of the bridging groups between the two copper ions in the complexes. As discussed above, the crucial steps of the mechanism earlier proposed³ is the cleavage of the OH bridge between the two metal ions and the subsequent proton transfer from the catechol substrate to the hydroxyl anion, leading to the release of one water molecule. It has been shown that the reaction of catechol with the complexes **1** and **2** does not result in a cleavage of the bridge, although the binding of the substrate to the chloride complex undoubtedly takes place. These results thus emphasize the influence of the bridging group between the copper centers on the catecholase activity of the complexes and underline the importance of the exogenous hydroxo bridge for the catalytic mechanism. This hydroxo ligand appears to be the key factor to achieve the complete deprotonation of catechol, leading to a bridging catecholate prior to the electron transfer. Upon substitution of the hydroxo bridge by a halogen anion, no proton transfer can occur, precluding the binding of catecholate in a didentate bridging fashion, and thus the subsequent catalytic cycle.

4.3 Experimental Section

4.3.1 Materials and Methods

All starting materials were commercially available and used as purchased. 2,6-bis(chloromethyl)-4-methylphenol was prepared as previously described.⁴ The NMR spectra were recorded on a JEOL FX-200 (200 MHz) FT-NMR spectrometer. The ligand field spectra of the solids (300-2000 cm⁻¹, diffuse reflectance) were taken on a Perkin-Elmer 330 spectrophotometer equipped with a data station. The ligand field spectra in solution were recorded on a Varian Cary 50 Scan UV-Vis spectrophotometer. Electrospray mass spectra (ESI-MS) in acetonitrile solutions were recorded on a Thermo Finnigan AQA apparatus. X-band electron paramagnetic resonance (EPR) measurements were performed at 77 K in the solid state on a Jeol RE2x electron spin resonance spectrometer, using DPPH ($g = 2.0036$) as a standard, and at 100 K as acetonitrile frozen solutions on a Bruker ESP 300E spectrometer operating at 9.4 GHz (X-band). The conductivity measurements were performed using a Philips PW9526 digital conductivity meter and a PW 9552/60 measuring cell with 0.5 mM solutions of the complexes in acetonitrile. The electrochemical behavior of the complexes was investigated in a 0.1 M solution of tetra-*n*-butylammonium perchlorate (TBAP) in acetonitrile using a EGG 273 potentiationstat coupled with a Kipp&Zonen x-y recorder. The experiments were performed at room temperature or at -40 °C in a three-compartment cell. Potentials are referred to an Ag/10 mM AgNO₃ + CH₃CN + 0.1 M TBAP reference electrode. The working electrode was a platinum disk of 5 mm diameter for the cyclic voltammetry (CV, 0.1 V/s) experiments or 3 mm diameter for the rotating disk electrode (RDE, 600 rpm) voltammetry experiments. The working

electrode was polished with 1 μm diamond paste prior to each recording. Bulk magnetizations of polycrystalline samples were performed on the crystals of the complexes **1** (11.11 mg) and **2** (16.88 mg) in the temperature range 5–400 K with a Quantum Design MPMS-5S SQUID magnetometer, in a 1 kG applied field. The data were corrected for the experimentally determined contribution of the sample holder. Corrections for the diamagnetic responses of the complexes, as estimated from Pascal's constants, were applied.²¹

4.3.2 Catecholase activity study

The catecholase activity of the complexes was evaluated by reaction with 3,5-di-*tert*-butylcatechol at 25 °C. The absorption at 400 nm, characteristic of the formed quinone, was measured as a function of time. The experiments were run under 1 atm of dioxygen. 3 ml of a $2.5 \cdot 10^{-4}$ M solution of complex in acetonitrile were placed in a 1 cm path-length cell, and 75 μl of a 1 M solution of the substrate in the same solvent were added. After thorough shaking, the changes in UV-Vis spectra were recorded during 30 min.

The titration of the complexes with tetrachlorocatechol (TCC) was carried out by adding 3 μl aliquots of a 0.1 M solution of TCC (corresponding to 0.198 eq of TCC/1 eq of the complex) to 3 ml of a $5 \cdot 10^{-4}$ M solution of complex in acetonitrile.

4.3.3 Ligand synthesis

***N*-(2-pyridylmethyl)-*N*-(2-thiophenylmethyl)amine:** A solution of 2.00 g (18.5 mmol) of 2-pyridylmethylamine was added dropwise upon stirring to a solution of 2.08 g (18.5 mmol) of 2-formylthiophene in MeOH. The resulting solution was stirred overnight at room temperature. Afterwards, 2.1 g (56 mmol, 3 eq per 1 CH=N) of NaBH₄ were added slowly, and the resulting solution was heated three hours at 50 °C. After evaporation of the solvent, the obtained oil was redissolved in a mixture of dichloromethane and water. The organic and aqueous layers were separated, and the water layer was washed twice with a small amount of dichloromethane. After drying the dichloromethane layer over Na₂SO₄ and evaporation under reduced pressure, the pure product was obtained as light yellow oil. The product is light-sensitive and should be preferably stored in the dark at low temperatures. Yield: 95%. ¹H NMR (CDCl₃, 200 MHz, ppm): δ = 2.28 (s, 1 H, NH); 3.95 (s, 2H, NHCH₂th); 4.03 (s, 2H, NHCH₂py); 6.93 (d, 1H, 3'th); 6.96 (s, 1H, 4'th); 7.20 (d, 1H, 5'th); 7.15 (t, 1H, 5'py); 7.30 (d, 1H, 3'py); 7.62 (t, 1H, 4'py); 8.55 (d, 1H, 6'py).

2,6-bis[*N*-(2-pyridylmethyl)-*N*-(2-thiophenylmethyl)aminomethyl]-4-methylphenol (Hpy2th2s): A solution of 0.7 g (3.4 mmol) of *N*-(2-pyridylmethyl)-*N*-(2-thiophenylmethyl)amine and 0.7 g (7 mmol) of Et₃N in THF was added dropwise upon stirring to a solution of 0.35 g (1.7 mmol) of 2,6-bis(chloromethyl)-4-methylphenol in THF. After refluxing for 2 hours, the solution was cooled to room

temperature. The filtration of the triethylammonium salt and the subsequent evaporation of the solvent resulted in an oil, which was dissolved in acidified water and washed with dichloromethane. The water layer was made alkaline by adding a concentrated aqueous solution of NH_3 , and the resulting suspension was extracted three times with dichloromethane. The organic layer was dried over Na_2SO_4 and evaporated under reduced pressure. The resulting oil was found to be the pure product. Yield: 84%. ^1H NMR (CDCl_3 , 200 MHz, ppm): δ = 2.28 (s, 3H, CH_3); 3.82 (s, 4H, NCH_2th); 3.85 (s, 4H, phCH_2N); 3.89 (s, 4H, NCH_2py); 6.95 (m, 4H, 3'th + 4'th), 7.04 (s, 2H, 3'ph + 5'ph); 7.15 (t, 2H, 5'th); 7.24 (d, 2H, 3'py); 7.53 (d, 2H, 5'th); 7.66 (t, 2H, 4'py); 8.56 (d, 2H, 6'py); 10.40 (1H, OH). ESI-MS: m/z 541 ($\text{M} + \text{H}^+$)

4.3.4 Syntheses of the coordination compounds

$[\text{Cu}_2(\text{py}2\text{th}2\text{s})(\mu\text{-Cl})\text{Cl}_2]\cdot\text{CH}_3\text{OH}$ (1): 0.15 g (0.28 mmol) of ligand Hpy2th2s and 0.10 g (0.54 mmol) of copper chloride were dissolved in 10 ml of methanol. Addition of 20 ml of diethyl ether resulted in the precipitation of the complex as a dark brown powder. Yield: 46% (102 mg). Single crystals of the complex were obtained by slow diffusion of diethyl ether into a 0.01 M solution of the complex. Elemental analysis, % found (calc.) for $[\text{Cu}_2(\text{py}2\text{th}2\text{s})(\mu\text{-Cl})\text{Cl}_2]\cdot\text{CH}_3\text{OH}$ ($= \text{C}_{32}\text{H}_{36}\text{Cl}_3\text{Cu}_2\text{N}_4\text{O}_2\text{S}_2$): C, 45.73 (47.73), H, 4.14 (4.38), N, 7.25 (6.96), S, 7.91 (7.96). ESI-MS: m/z 737 ($[\text{Cu}_2(\text{py}2\text{th}2\text{s})\text{Cl}_2]^+$)

$[\text{Cu}_2(\text{py}2\text{th}2\text{s})(\mu\text{-Br})\text{Br}_2]$ (2): 0.15 g (0.28 mmol) of ligand Hpy2th2s and 0.12 g (0.54 mmol) of copper bromide were dissolved in 10 ml of methanol. After addition of diethyl ether to the resulting solution, the complex precipitated as a dark-purple crystalline powder. Yield: 64% (155 mg). Crystals suitable for X-ray diffraction were obtained by slow diffusion of diethyl ether into a 0.01 M solution of the complex in acetonitrile. Elemental analysis, % found (calc.) for $[\text{Cu}_2(\text{py}2\text{th}2\text{s})(\mu\text{-Br})\text{Br}_2]$ ($= \text{C}_{31}\text{H}_{32}\text{Br}_3\text{Cu}_2\text{N}_4\text{OS}_2$): C, 39.76 (40.95), H, 3.42 (3.76), N, 6.07 (5.97), S, 6.50 (6.83). ESI-MS: m/z 827 ($[\text{Cu}_2(\text{py}2\text{th}2\text{s})\text{Br}_2]^+$)

4.3.5 X-ray crystallographic measurements

$[\text{Cu}_2(\text{py}2\text{th}2\text{s})(\mu\text{-Cl})\text{Cl}_2]\cdot\text{CH}_3\text{OH}$ (1): A single crystal of $[\text{Cu}_2(\text{py}2\text{th}2\text{s})(\mu\text{-Cl})\text{Cl}_2]\cdot\text{CH}_3\text{OH}$ (1) was mounted at 150 K on a Bruker AXS SMART 6000 diffractometer equipped with Cu-K α radiation ($\lambda = 1.54184$ Å). $\text{C}_{32}\text{H}_{36}\text{Cu}_2\text{N}_4\text{O}_2\text{S}_2\text{Cl}_3$, Fw = 802.17, rectangular reddish-brown plates, $0.23 \times 0.21 \times 0.05$ mm, $a = 7.984(2)$, $b = 34.589(7)$, $c = 12.554(3)$ Å, $\beta = 94.31(3)^\circ$, $Z = 4$, $V = 3457(2)$ Å³, monoclinic, space group $P2_1/n$ (no. 14), $\rho_{\text{calc.}} = 1.541$ g cm⁻³, $\mu = 5.068$ mm⁻¹, absorption correction: SADABS,²² reflections collected: 19864, independent reflections: 6317 ($R_{\text{int}} = 0.0386$). The structure was solved by direct methods and refined using the SHELX program package.^{23,24} All hydrogen atoms were placed on idealized positions riding on the carrier atom, with isotropic displacement parameters. The final cycle of full-matrix least-

squares refinement, including 438 parameters, converted to $R1 = 0.0352$ ($R1 = 0.0430$ all data) and $wR2 = 0.1009$ ($wR2 = 0.1038$ all data) with a maximum (minimum) residual electron density of 0.535 (-0.466) $\text{e} \text{ \AA}^{-3}$.

[Cu₂(py2th2s)(μ -Br)Br₂] (2): C₃₁H₃₁Br₃Cu₂N₄OS₂ + solvent, Fw = 906.53, red needle, $0.60 \times 0.06 \times 0.03 \text{ mm}^3$, triclinic, $P\bar{1}$ (no. 2), $a = 8.4207(2)$, $b = 17.9812(4)$, $c = 24.2238(6) \text{ \AA}$, $\alpha = 71.2709(9)$, $\beta = 81.2708(7)$, $\gamma = 80.6146(11)^\circ$, $V = 3407.66(14) \text{ \AA}^3$, $Z = 4$, $\rho_{\text{calc.}} = 1.767 \text{ g cm}^{-3}$, 43713 measured reflections, 12061 unique reflections ($R_{\text{int}} = 0.0734$), 8080 observed reflections [$I > 2\sigma(I)$]. 775 refined parameters, no restraints. R (obs. refl.): $R1 = 0.0461$, $wR2 = 0.1121$. R (all data): $R1 = 0.0776$, $wR2 = 0.1286$. $S = 1.085$. Residual electron density between -1.08 and 1.17 e/\AA^3 . Intensities were measured on a Nonius KappaCCD diffractometer with rotating anode (Mo-K α , $\lambda = 0.71073 \text{ \AA}$) at a temperature of 150 K. An absorption correction based on multiple measured reflections was applied ($\mu = 4.920 \text{ mm}^{-1}$, 0.59-0.86 transmission). The structure was solved with direct methods using the program SHELXS97,²⁵ and refined with the program SHELXL97²⁴ against F^2 of all reflections up to a resolution of $(\sin \theta/\lambda)_{\text{max}} = 0.60 \text{ \AA}^{-1}$. Non-hydrogen atoms were refined freely with anisotropic displacement parameters. Hydrogen atoms were refined as rigid groups. Three of the thiophene rings were rotationally disordered and refined with occupancies of 0.85:0.15, 0.72:0.28, and 0.55:0.45, respectively. The crystal structure contains large voids ($150.9 \text{ \AA}^3/\text{unit cell}$) filled with disordered solvent molecules. Their contribution to the structure factors was secured by back-Fourier transformation (program PLATON,²⁶ CALC SQUEEZE, $22 \text{ e}^-/\text{unit cell}$). The drawings, structure calculations, and checking for higher symmetry was performed with the program PLATON.²⁶

CCDC-230014 (compound **1**) and 230015 (compound **2**) contain the supplementary crystallographic data for this chapter. These data can be obtained free of charge at www.ccdc.cam.ac.uk/conts/retrieving.html [or from the Cambridge Crystallographic Data Centre, 12, Union Road, Cambridge CB2 1EZ, UK; fax: (internat.) +44-1223/336-033; E-mail: deposit@ccdc.cam.ac.uk].

4.4 References

- (1) Klabunde, T.; Eicken, C.; Sacchettini, J. C.; Krebs, B. *Nat. Struct. Biol.* **1998**, *5*, 1084-1090.
- (2) Merkel, M.; Möller, N.; Piacenza, M.; Grimme, S.; Rompel, A.; Krebs, B. *Chem. Eur. J.* **2005**, *11*, 1201-1209.
- (3) Torelli, S.; Belle, C.; Hamman, S.; Pierre, J. L.; Saint-Aman, E. *Inorg. Chem.* **2002**, *41*, 3983-3989.
- (4) Borovik, A. S.; Papaefthymiou, V.; Taylor, L. F.; Anderson, O. P.; Que, L. *J. Am. Chem. Soc.* **1989**, *111*, 6183-6195.
- (5) Addison, A. W.; Rao, T. N.; Reedijk, J.; van Rijn, J.; Verschoor, G. C. *J. Chem. Soc., Dalton Trans.* **1984**, 1349-1356.
- (6) Torelli, S.; Belle, C.; Gautier-Luneau, I.; Pierre, J. L.; Saint-Aman, E.; Latour, J. M.; Le Pape, L.; Luneau, D. *Inorg. Chem.* **2000**, *39*, 3526-3536.
- (7) Rajendran, U.; Viswanathan, R.; Palaniandavas, M.; Laskiminaraya, N. *J. Chem. Soc., Dalton Trans.* **1994**, 1219-1226.
- (8) Ruiz, E.; Alemany, P.; Alvarez, S.; Cano, J. *J. Am. Chem. Soc.* **1997**, *119*, 1297-1303.
- (9) Bertoncello, K.; Fallon, G. D.; Hodgkin, J. H.; Murray, K. S. *Inorg. Chem.* **1988**, *27*, 4750-4758.

- (10) Sorrel, T. N.; O'Connor, C. J.; Anderson, O. P.; Reibenspies, J. H. *J. Am. Chem. Soc.* **1985**, *107*, 4199-4206.
- (11) Belle, C.; Beguin, C.; Gautier-Luneau, I.; Hamman, S.; Philouze, C.; Pierre, J. L.; Thomas, F.; Torelli, S.; Saint-Aman, E.; Bonin, M. *Inorg. Chem.* **2002**, 479-491.
- (12) Geary, W. J. *Coord. Chem. Rev.* **1971**, *7*, 81-122.
- (13) Walton, R. A. *Quart. Rev.* **1965**, *19*, 126-143.
- (14) Reim, J.; Krebs, B. *J. Chem. Soc., Dalton Trans.* **1997**, 3793-3804.
- (15) Börzel, H.; Comba, P.; Pritzkow, H. *Chem. Commun.* **2001**, 97-98.
- (16) Karlin, K. D.; Gultneh, Y.; Nicholson, T.; Zubieta, J. *Inorg. Chem.* **1985**, *24*, 3725-3727.
- (17) Fernandes, C.; Neves, A.; Bortoluzzi, A. J.; Mangrich, A. S.; Rentschler, E.; Szpoganicz, B.; Schwingel, E. *Inorg. Chim. Acta* **2001**, *320*, 12-21.
- (18) Kao, C.-H.; Wei, H.-H.; Liu, Y.-H.; Lee, G.-H.; Wang, Y.; Lee, C.-J. *J. Inorg. Biochem.* **2001**, *84*, 171-178.
- (19) Neves, A.; Rossi, L. M.; Bortoluzzi, A. J.; Szpoganicz, B.; Wiezbicki, C.; Schwingel, E.; Haase, W.; Ostrovsky, S. *Inorg. Chem.* **2002**, *41*, 1788-1794.
- (20) Mukherjee, J.; Mukherjee, R. *Inorg. Chim. Acta* **2002**, *337*, 429-438.
- (21) Kolthoff, I. M.; Elving, P. J. *Treatise on Analytical Chemistry*; Interscience Encyclopedia, Inc.: New York, 1963.
- (22) Bruker AXS Inc., Madison, WI, 1999.
- (23) Sheldrick, G. M.; *SHELXTL PLUS*. University of Göttingen, Germany, 1990
- (24) Sheldrick, G. M.; *SHELXL-97, Program for the refinement of crystal structures*. University of Göttingen, Germany, 1997
- (25) Sheldrick, G. M.; *SHELXS-97, Program for crystal structure solution*. University of Göttingen, Germany, 1997
- (26) Spek, A. L. *J. Appl. Cryst.* **2003**, *36*, 7-13.

